13th IEA Heat Pump Conference
April 26-29, 2021 Jeju, Korea

Effectiveness-based air flow rate optimization for a residential heat pump in seasonal performance conditions

Minsu Park[a], Min Soo Kim[b*]

[a]LG Electronics Corp., 128 Yeouidae-ro, Yeongdeungpo-gu, Seoul 07736, Republic of Korea
[b]Seoul National University, 1 Gwanak-ro, Gwanak-gu, Seoul 08826, Republic of Korea

Abstract

The conventional rating performance of a residential heat pump system is being replaced by the seasonal performance due to increased demands for the energy saving. In order to achieve the satisfactory seasonal performance, the current system should be modified according to the part load characteristics. Moreover, operating conditions of actuators must be optimized for each test condition to acquire the utmost system efficiency. Fan speeds of both indoor and outdoor units are one of the most significant variable since they are individually controllable and the operating ranges of them are broad. Hence, in this study, effectiveness-based simulation model is introduced to accurately predict the optimum air flow of the system for each seasonal performance condition. The heat exchanger performance is predicted by the modified effectiveness, which can be obtained from the developed non-dimensional correlation. The compressor performance is estimated by the semi-empirical efficiency models. From the verification result, the developed model can estimate the optimum air flow rate within an error of 10% for seasonal performance conditions.

Selection and/or peer-review under responsibility of the organizers of the 13th IEA Heat Pump Conference 2020.

Keywords: Residential heat pump; Seasonal energy efficiency ratio (SEER); Seasonal coefficient of performance (SCOP); Modified effectiveness; Air flow rate;

1. Introduction

The amount of energy consumed by HVAC system is the large part of total power supply and thus demands for the high efficiency system have been constantly increased. Heat pump is considered as one of the most efficient device so many researches have been conducted for the performance improvement. Conventional researches have concentrated on the rating performance but seasonal performance is being more important due to the rising usage of an inverter compressor. Therefore, new performance index is required to represent the overall performance in various part load conditions, so European Union introduced the new energy label for SEER and SCOP [1]. As a result, consumers are not interested in the rating efficiency any more but consider the energy grade for seasonal efficiency and thus manufacturers are now focusing on improving seasonal performance. Regarding SEER and SCOP, part load efficiency is significant for seasonal performance so it is inevitable to optimize current system according to part load characteristics [2].

Regarding a compressor, it is required to secure better performance in part load conditions, so the accurate estimation of the efficiency is essential for various operating conditions. For this reason, many researchers tried to estimate compressor efficiencies with various methods. Ishii et al. numerically examined the net efficiency for various geometry [3] and Yang et al. established a model for volumetric and isentropic efficiency with neural network method [4]. Dutra and Deshamps developed an induction motor model for motor efficiency [5]. However, stated models are not appropriate to be applied for any compressor since they are only

* Corresponding author. Tel.: +82-2-880-8362; fax:.
E-mail address: minskim@snu.ac.kr.

valid for the certain compressor. Therefore, semi-empirical efficiency models are developed for the compressor installed in the reference system shown in Table 1.

Regarding a heat exchanger, it is essential to reduce air side thermal resistance for better performance but this enhancement generally augments air side pressure drop [6]. As a result, COP can be deteriorated due to the increased fan power consumption, especially at the low load conditions. Thus, it is required to consider both air side hA and pressure drop for each part load condition. In other words, the optimum air flow rate of each heat transfer condition should be defined to maximize the heat exchanger performance. Lee et al. introduced the simulation-based solution with utilizing genetic algorithm and identified the big difference between the optimized and non-optimized air flow rate under seasonal performance conditions [7]. However, new dataset will be required if specifications of the system are changed. Thus, the author established the simulation model to easily obtain required performance data but it still takes considerable time since iteration processes are included. The calculation time can be drastically increased as iteration loops should be repeatedly conducted for various indoor and outdoor air flow rates. Furthermore, correction factors should be appropriately selected for each correlation to accurately calculate the heat exchanger performance if geometries are changed. The model that has many iteration loops or needs updates for changeable specifications will not be appropriate for a commercial system considering the practical capability of a MiCom in the system.

Hence, this study investigates the non-iterative and universal solution to optimize both indoor and outdoor air flow rates for seasonal performance conditions. The developed model can instantly predict the optimum air flow rate and its accuracy is validated by experiments.

2. Model description

2.1. Heat exchanger model

The modified effectiveness is newly proposed to calculate both sensible and latent heat transfer rate for various heat exchanger geometries. In case of a heat exchanger of the refrigerant cycle, the actual and the maximum heat transfer rate can be expressed as the following Eqs. (1) and (2) [8]. Only two-phase heat transfer is considered for the refrigerant side since the heat transfer mainly occurs at that region. The temperature at the halfway point of a single path is considered as the $T_{ref,sat}$ and the effectiveness for dry condition can be expressed as Eq. (3) for dry condition.

$$Q_{actual} = C_c\left|T_{c,i} - T_{c,o}\right| = \dot{m}_{a,ID} C_{p,a,ID}\left|T_{a,ID,i} - T_{a,ID,o}\right| \tag{1}$$

$$Q_{max} = C_{min}\left|T_{h,i} - T_{c,o}\right| = \dot{m}_{a,ID} C_{p,a,ID}\left|T_{ref,sat} - T_{a,ID,i}\right| \tag{2}$$

$$\varepsilon_{dry} = \frac{Q_{actual}}{Q_{max}} = \frac{\Delta T_a}{\left|T_{ref,sat} - T_{a,i}\right|} \tag{3}$$

Table 1. Specifications of the reference system

Model		AS-W126M, LG Electronics
Performance	Rating capacity [kW]	3.5 for cooling, 4.0 for heating
	Rating COP	4.22 for cooling, 5.19 for heating
	Pdesign [kW]	3.5 for cooling, 3.8 for heating
	SEER	8.5 (A+++)
	SCOP	5.1 (A+++)
Outdoor Unit	Compressor	12.8 cc Twin Rotary
		DA128A1FA-20F, Toshiba
	Heat exchanger	Fin and tube, Φ7, 2 Rows, 814 mm
	Fan	Axial, BLDC motor
	EEV	Φ 1.65 mm orifice, Sanhua
Indoor Unit	Heat exchanger	Fin and tube, Φ7, 3 Rows, 680 mm
	Fan	Cross flow, BLDC motor
Refrigerant		R410A, 1.0 kg

Table 2. Specifications of heat exchangers

	#1	#2	#3
Fin type	Slit	Slit	Corrugated
Number of rows	3	3	2
Number of steps	16	24	24
FPI	21	22	18
D_o [mm]	7.35	5.20	7.35
L [mm]	680	740	814
P_R [mm]	12.7	10.0	18.2
P_S [mm]	21	14	21

In case of wet condition, the effectiveness cannot be acquired by the temperature difference due to the latent heat, so the effectiveness is defined as the ratio of the actual to the maximum enthalpy difference of air [9]. In order to obtain h_{max}, the enthalpy of the outlet air is assumed to be the smallest when the air wet bulb temperature is equal to the evaporating temperature. The effectiveness can be expressed as Eq. (4) for wet condition.

$$\varepsilon_{wet} = \frac{h_{actual}}{h_{max}} = \frac{\Delta h_a}{h_{a,i} - h_{a,min}} \tag{4}$$

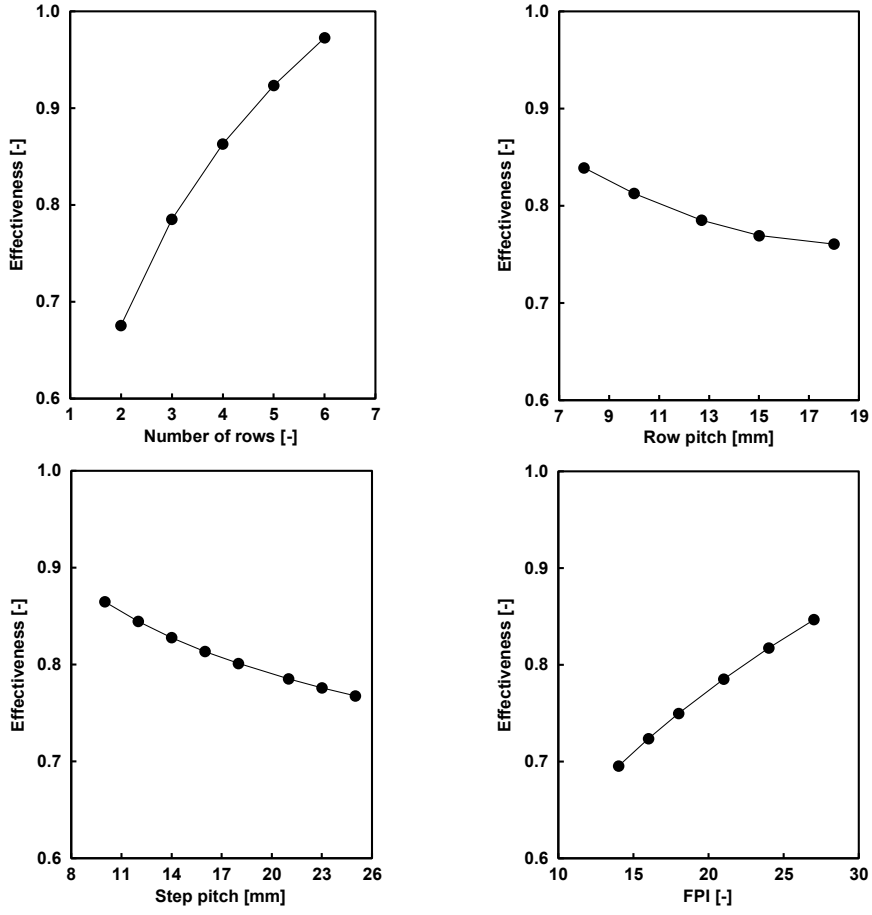

Fig. 1. Variation of the modified effectiveness for various heat exchanger geometry

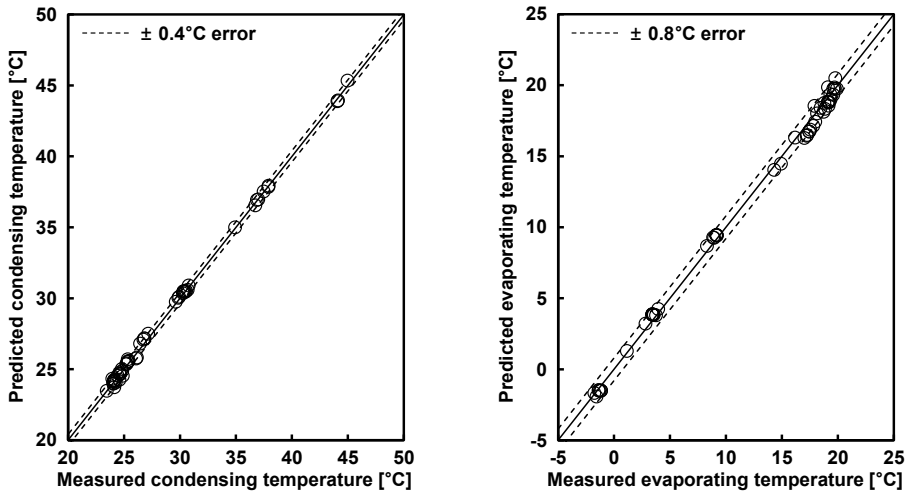

Fig. 2. Validation for saturation temperatures

Heat exchangers were selected as described in Table 2 and experimental data were obtained for each heat exchanger to establish the correlation between the effectiveness and various geometries of the heat exchanger. Key factors are selected by data analysis and the effect on the effectiveness is examined for each factor. Consequently, a non-dimensional correlation for the modified effectiveness which represents both ε_{dry} and ε_{wet} is developed as Eq. (5). α is 1.00 for the corrugated fin and 1.06 for the slit and louvered fin, while β is -0.02 for condensation and 0.02 for evaporation. The root mean square (RMS) error of the developed model is 2.7% for condensation and 5.3% for evaporation. Hence, this correlation can accurately predict the modified effectiveness for heat exchangers which have various geometries. Fig. 1 shows the variation of the effectiveness for number of rows, row pitch, step pitch and FPI, respectively.

$$\varepsilon = 0.43\alpha(0.2644\ln R + 0.4761)\left(\frac{P_r}{P_f}\right)^{0.3}\left(\frac{P_r}{P^*}\right)^{-0.35}\left(\frac{P^*}{P_s}\right)^{0.02\left(\frac{P_r}{D_c}\right)^{3.6}} PLR^{\beta}(1-0.00025\mathrm{Re_D}) \quad (5)$$

Capacity can be fixed for each seasonal performance condition since the inverter compressor will be operated to match the part load. Thus, heat transfer rate of the indoor heat exchanger can be the input and the heat transfer rate of the outdoor heat exchanger can be calculated by Eqs. (6) and (7). Temperature and enthalpy difference of air side can be acquired by Eqs. (1) and (8), respectively. As a result, saturation temperatures of the refrigerant can be attained without an iteration process from the modified effectiveness. The RMS error of the predicted condensing temperature is only 0.19°C while 0.41°C for evaporating temperature as shown in Fig. 2.

$$Q_{OD,c} = Q_{ID}(1 + 0.18PLR^{1.3}) \quad (6)$$

$$Q_{OD,h} = Q_{ID}/(1 + 0.08PLR^{1.16}) \quad (7)$$

$$Q_e = \dot{m}_a(h_{a,i} - h_{a,o}) \quad (8)$$

In addition, in order to estimate the power consumption of both indoor and outdoor fans, the empirical polynomial equations are established from the pressure to volume flow rate data provided by the manufacturer.

Table 3. Compressor coefficients

V_0	V_1	V_2	V_3	V_4	M_0	M_1	M_2	M_3	M_4
1.1160	-0.0764	0.2934	0.0006	-0.0351	0.6944	-0.0001	0.0171	-0.1619	-0.0010

2.2. Compressor model

In order to determine the optimum air flow rate, compressor power should be accurately calculated since it is the largest part of the power consumption. If experimental data is attainable for the whole operating range, map-based model will be effective. However, it is unavailable to conduct the experiment when rotational speed of a compressor is very low. Furthermore, the excessive DSH should be maintained at the compressor suction according to the compressor performance standards. Hence, map-based model is inapposite for part load conditions and thus efficiency-based model is applied for the compressor. Semi-empirical correlations are developed as the following Eqs. (9) to (13) for isentropic, volumetric and mechanical efficiency. Regarding Eqs. (12) and (13), several coefficients are applied to reflect various specifications of a compressor and coefficients for the reference system are indicated in Table 3. RMS error of the developed correlation is 5.6% for η_{isen}, 3.1% for η_{vol} and 6.3% for η_{mech} including motor and drive efficiencies.

$$\eta_{isen,c} = -0.0782\Theta^2 + 0.4121\Theta + 0.3297 \tag{9}$$

$$\eta_{isen,h} = -0.0261\Theta^2 + 0.2060\Theta + 0.5905 \tag{10}$$

where

$$\Theta = \frac{T_{dis,ideal} - T_{a,OD,i}}{2\pi N \cdot 3600 \cdot V_{disp} \cdot PR} \tag{11}$$

$$\eta_{vol} = V_0 + V_1 PR^2 + V_2 PR + V_3 \rho_{suc}^2 + V_4 \rho_{suc} \tag{12}$$

$$\eta_{mech} = M_0 + M_1 N^2 + M_2 N + M_3 PR + M_4 T_{a,OD,i} \tag{13}$$

3. Experiments

3.1. Experimental setup

Experiments are conducted in the calorimeter consists of the indoor and the outdoor chambers to verify the established simulation model. The wind tunnel is installed in the indoor chamber to measure the capacity of the indoor unit by air-enthalpy method. Temperature and humidity are steadily maintained by air handling units, so that deviations of every air temperature are less than ± 0.1°C from each set value. The air flow rate of the indoor unit is acquired by the differential pressure sensor at the nozzle.

Table 4 shows test conditions of EN 14825 and SCOP A, E and F are excluded since these conditions are insignificant on SCOP. Experiments are carried out with various indoor air flow rates and outdoor fan speeds for each test condition to determine the optimum air flow rate. Compressor speed is controlled to make the capacity correspond to the part load for each condition and EEV is adjusted to maintain DSH at the evaporator outlet as 1°C for all conditions. In D conditions of both SEER and SCOP, COP will be degraded by the following Eq. (14) since the capacity substantially exceeds the part load even though the compressor operates at the lowest rotational speed [1].

Table 4. Test conditions

		PLR [%]	Outdoor DBT / WBT [°C]	Indoor DBT / WBT [°C]
SEER	A	100	35 / 24	27 / 19
	B	74	30 / 20	27 / 19
	C	47	25 / 16	27 / 19
	D	21	20 / 12	27 / 19
Heating	Rating	100	7 / 6	20 / 15
SCOP	B	54	2 / 1	20 / 15
	C	35	7 / 6	20 / 15
	D	15	12 / 11	20 / 15

$$COP_d = COP(1 - C_d(1 - Q_{rating}/Q_{measured})) \quad (14)$$

3.2. Data reduction

The measurement data is obtained at the complete steady-state according to the standard [10] and both capacity and COP are calculated by the following Eqs. (15) to (18). The latent heat is not considered if the air speed is significantly high since condensation does not occur in the evaporator.

$$Q_{a,c} = \dot{m}_{a,ID}(h_{a,ID,i} - h_{a,ID,o}) + KA_{WT,surf}(T_{a,ID,i} - T_{a,ID,o}) \quad (15)$$

$$Q_{a,c,SH} = \dot{m}_{a,ID}\, C_{p,a,ID}(T_{a,ID,i} - T_{a,ID,o}) + KA_{WT,surf}(T_{a,ID,i} - T_{a,ID,o}) \quad (16)$$

$$Q_{a,h} = \dot{m}_{a,ID}\, C_{p,a,ID}(T_{a,ID,o} - T_{a,ID,i}) + KA_{WT,surf}(T_{a,ID,o} - T_{a,ID,i}) \quad (17)$$

$$COP = Q_a/W \quad (18)$$

3.3. Uncertainty analysis

Uncertainty of the acquired data is shown in Table 5 and its propagation is indicated in Table 6. In order to analyze the uncertainty of the cooling capacity and COP, the uncertainty of the air enthalpy should be examined. However, it cannot be directly measured by sensors but can be calculated by temperatures or humidity. Generally, it can be obtained by measured dry bulb and wet bulb temperature through the complicated calculating process which is not appropriated for the uncertainty analysis. Therefore a linear formula is developed as Eq. (19) within the measurable range, so the propagated error of the cooling capacity and COP can be calculated as the following Eqs. (20) to (22) for every test condition [11]. If the condensation does not occur, it is recommended to only consider sensible heat to reduce the error since the uncertainty of the air enthalpy difference is crucially larger than that of the temperature difference. As a result, the uncertainty is 2.0 ~ 4.3% for cooling COP and 1.8 ~ 2.6% for heating COP which are deserved to be reliable.

$$h_a = -0.0437\, T_{DB} + 3.160 T_{WB} - 4.508 \quad (19)$$

$$\frac{U_{h_a}}{h_a} = \sqrt{\left(\frac{\partial h_a}{\partial T_{DB}}\right)^2 + \left(\frac{\partial h_a}{\partial T_{WB}}\right)^2} \quad (20)$$

$$\frac{U_{COP_c}}{COP_c} = \sqrt{\left(\frac{U_{\dot{m}_a}}{\dot{m}_a}\right)^2 + \left(\frac{U_{\Delta h_a}}{\Delta h_a}\right)^2 + \left(\frac{U_W}{W}\right)^2} \quad (21)$$

$$\frac{U_{COP_h}}{COP_h} = \sqrt{\left(\frac{U_{\dot{m}_a}}{\dot{m}_a}\right)^2 + \left(\frac{U_{\Delta T}}{\Delta T}\right)^2 + \left(\frac{U_W}{W}\right)^2} \quad (22)$$

Table 5. Uncertainty analysis

Measurable value		Uncertainty
Indoor air inlet dry bulb temperature	[°C]	0.04
Indoor air inlet wet bulb temperature	[°C]	0.08
Indoor air outlet dry bulb temperature	[°C]	0.05
Indoor air outlet wet bulb temperature	[°C]	0.07
Outdoor air inlet dry bulb temperature	[°C]	0.03
Outdoor air inlet wet bulb temperature	[°C]	0.06
Indoor air outlet Nozzle ΔP	[%]	0.10
Power consumption	[%]	0.20

Table 6. Error propagation analysis

For cooling condition		A	B	C	D
Air mass flow rate	[%]	1.67	1.67	1.67	1.67
Inlet air enthalpy	[kJ kg^{-1}]	0.25	0.25	0.25	0.25
Outlet air enthalpy	[kJ kg^{-1}]	0.22	0.22	0.22	0.22
Enthalpy difference	[%]	2.95	3.92	4.95	5.55
Temperature difference	[%]	-	-	0.91	1.07
Capacity	[%]	3.39	4.26	1.90	1.98
COP	[%]	3.43	4.29	2.21	2.03
For heating condition			B	C	D
Air mass flow rate	[%]		1.67	1.67	1.67
Temperature difference	[%]		1.07	1.28	1.60
Capacity	[%]		1.98	2.10	2.31
COP	[%]		2.08	2.58	2.35

4. Result analysis

The optimum indoor and outdoor air speeds of each seasonal performance condition are obtained by the established simulation model and validated by measured data. In order to obtain the optimum air flow rate via simulation, wide range of air speed is given and then COP is promptly calculated for each air speed without any iteration process. The optimum air speed can be ascertained for each seasonal performance condition from the results. Detailed simulation results for both indoor and outdoor heat exchangers are indicated in Table 7 and it is obvious that each operating condition has its own optimum air speed that can achieve the best performance. The optimum air speed has a positive correlation with the capacity but the tendency is slightly different for indoor and outdoor heat exchanger. The indoor heat exchanger is more influenced by the cooling capacity while the outdoor heat exchanger is more affected by the heating capacity, which identifies that the air flow rate of the evaporator is less influential for the performance.

In order to examine the stated correlation between the optimum air speed and the capacity, distribution of the power consumption should be firstly considered. The power consumption of the compressor is more than 80% of the total at the full load condition, so it can be advantageous to increase the air flow rate to reduce the pressure ratio of the compressor. However, at the low load condition, it will be reduced under 60% and hence the power consumption of both fans is about 30% instead. Therefore, COP can be significantly decreased when the air speed is not well optimized. For instance, COP will be deteriorated by 10% in SEER D condition if the indoor air flow rate is 75% of the optimum value but it will decline by only 1% in SEER A condition. In fact, in order to achieve the remarkable seasonal performance, it is essential to operate the system at the optimum air speed. Secondly, the suitable air side temperature difference should be secured for the thermal comfort of occupants, so UA of the indoor heat exchanger is generally smaller than that of the outdoor heat exchanger. In addition, both sensible and latent heat exist at the evaporator, the air flow rate can be less influential since the

Table 7. Verification results

Test condition		Optimum indoor air flow rate [CMM]			Optimum outdoor air flow rate [CMM]		
		Predicted	Measured	Error	Predicted	Measured	Error
SEER	A	24.0*	15.5	+ 54.8%	39.4*	32.6	+ 20.9%
	B	18.5*	15.5	+ 19.4%	32.0	32.2	- 0.6%
	C	13.0	12.5	+ 4.0%	24.6	25.9	- 5.0%
	D	10.3	10.0	+ 3.0%	20.9	19.5	+ 7.2%
SCOP	B	14.4	14.5	- 0.7%	23.4	23.7	- 1.3%
	C	11.7	11.5	+ 1.7%	16.0	17.2	- 7.0%
	D	10.3	10.0	+ 3.0%	13.5	15.0	- 10.0%

* Above the permissible sound pressure level

reduced temperature difference between the fin surface and the moist air will decrease the latent heat which has the exceedingly large enthalpy difference. Consequently, the decreasing tendency of the optimum air flow rate according to the capacity is differently observed for indoor and outdoor heat exchanger as well as cooling and heating operation. Therefore, the optimum air flow rate should be separately investigated by considering the heat transfer circumstance of the heat exchanger.

Simulation results are validated by the experimental results and described in Table 7. In some cases, the air flow rate cannot reach the predicted optimum value even though fan motor is operated at its maximum speed. Practically, the air flow rate should be regulated to satisfy the noise regulation, so maximum speed of the motor is designed around the limit value. Thus, results cannot be obtained for the air flow rate which exceeds the maximum speed nevertheless the optimum COP is not identified within the experimental data. As a result, the modeling shows an unusual large error for those test conditions. However, it can precisely predict the optimum air flow rate with the RMS error of 4.9%, 2.7% for the indoor air flow rate and 6.2% for the outdoor air flow rate. Furthermore, if the real-time capacity can be secured during heat pump operation, the optimum air flow rate of both indoor and outdoor units will be instantly obtained for the current operating condition. In fact, the system can be operated with the optimum air flow rate all the time, which implies the most practical energy saving.

5. Conclusion

In this study, effectiveness-based simulation model is established to accurately predict the optimum air flow rate for various operating conditions. The non-dimensional correlation which can reflect various heat exchanger geometries is introduced for the modified effectiveness, so COP can be ascertained for various air flow rate and load conditions. The correlation can predict the condensing and evaporating temperature within the RMS error of 2.7% and 5.3%, respectively. Furthermore, the optimum air flow rate of various seasonal performance test conditions can be predicted within the RMS error of 4.9% for the permissible operation range of both fans. If the system is available to calculate its real-time capacity, the utmost COP can be always secured by predicting the optimum air flow rate for the calculated capacity.

Acknowledgements

This research is supported by the Institute of Advanced Machinery and Design (IAMD) and Institute of Engineering Research (IER) of Seoul National University. Supports from the Brain Korea 21 Plus Project (F14SN02D1310) of the Ministry of Education and the Basic Science Research Program through the National Research Foundation (NRF) of the Ministry of Science, ICT & Future Planning (2016R1A2A1A05005510) are appreciated. The program of the Korea Institute of Energy Technology Evaluation and Planning (KETEP) from the Ministry of Trade, Industry & Energy of Korea (No. 20173010032150) is also appreciated. Support from the R&D Center for reduction of Non-CO2 Greenhouse gases (2017002430001) funded by Korea Ministry of Environment (MOE) as Global Top Environment R&D Program is sincerely recognized.

References

[1] EN 14825, 2013. Air conditioners, liquid chilling packages and heat pumps, with electrically driven compressors, for space heating and cooling – Testing and rating at part load conditions and calculation of seasonal performance. British Standards Institution, London, U.K.

[2] Kinab, E., Marchio, D., Reviere, P., 2010. Reversible heat pump model for seasonal performance optimization. Energy and Buildings 42, p. 2269-2280.

[3] Ishii, N., Morita, N., Ono, M., Yamamoto, S., Sano, K., 2000. Net efficiency simulations of compact rotary compressors for its optimal performance. International Compressor Engineering Conference 1424, p. 475-482.

[4] Yang, L., Zhao, L., Zhang, C., Gu, B., 2009. Loss-efficiency model of single and variable-speed compressors using neural networks. International Journal of Refrigeration 32, p. 1423-1432.

[5] Dutra, T., Deschamps, C. J., 2015. A simulation approach for hermetic reciprocating compressors including electrical motor modeling. International Journal of Refrigeration 59, p. 168-181.

[6] Fischer, S.K., Rice, C.K., 1983. The Oak Ridge heat pump models: I. A Steady-state computer design model for air-to-air heat pumps. Oak Ridge National Laboratory, Tennessee.

[7] Lee, S., Jeon, Y., Chung, H., Cho, W., Kim, Y., 2018. Simulation-based optimization of heating and cooling seasonal performances of an air-to-air heat pump considering operating and design parameters using genetic algorithm. Applied Thermal Engineering 144, 362-370.
[8] Incropera, F. P., DeWitt, D., 2002. Fundamentals of Heat and Mass Transfer, 5th ed. Wiley, New York.
[9] Mansour, M. K., 2016. Practical effectiveness-NTU model for cooling and dehumidifying coil with non-unit Lewis Factor. Applied Thermal Engineering 100, p. 1111~1118
[10] EN 14511-3, 2013. Air conditioners, liquid chilling packages and heat pumps with electrically driven compressors for space heating and cooling – Part 3: Test methods. British Standards Institution, London, U.K.
[11] ASHRAE Guideline 2-2010, 2014. Engineering analysis for experimental data. ASHRAE, Atlanta, GA.

Nomenclature

$A_{WT,\,surf}$	surface area of the wind tunnel [m^2]
C_p	specific heat [kJ kg^{-1} K^{-1}]
C_d	degradation coefficient
COP	coefficient of performance
Dc	fin collar diameter [mm]
DSH	degree of superheat [°C]
ε	effectiveness of a heat exchanger
h	enthalpy [kJ kg^{-1}]
K	heat transmission coefficient [W m^{-2} K^{-1}]
$\dot{m}$	mass flow rate [kg h^{-1}]
N	rotational speed of a compressor [Hz]
P	pitch [mm]
*P**	reference pitch, 25.4 [mm]
PLR	part load ratio
PR	pressure ratio
Q	transferred heat [kW]
R	number of rows
Re_D	Reynolds number based on fin collar diameter
SCOP	seasonal coefficient of performance
SEER	seasonal energy efficiency ratio
T	temperature [°C]
U	uncertainty
$\dot{V}$	volume flow rate [m^3 min^{-1}]
V_{disp}	compressor displacement [cc]
W	work [W]
Δh	enthalpy difference [kJ kg^{-1}]
ΔT	temperature difference [°C]
η	compressor efficiency
ρ	density [kg m^{-3}]

Subscripts

a	air side
c	cooling
DB	dry bulb
dis	discharge
e	evaporating
f	fin
h	heating
i	inlet
ID	indoor unit
isen	isentropic
max	maximum
mech	mechanical
min	minimum
o	outlet
OD	outdoor unit
r	row
ref	refrigerant
s	step
sat	saturation
SH	sensible heat
suc	suction
vol	volumetric
WB	wet bulb